Langmuir

Article

pubs.acs.org/Langmuir

Using DNA-Driven Assembled Phospholipid Nanodiscs as a Scaffold for Gold Nanoparticle Patterning

Nienke Geerts,[†] Carl F. Schreck,[§,∥] Paul A. Beales,[‡] Hideki Shigematsu,[#] Corey S. O'Hern,[§,∥,⊥] and T. Kyle Vanderlick*[,†]

[†]Chemical & Environmental Engineering, Yale University, New Haven, Connecticut 06511, United States

[‡]Centre for Molecular Nanoscience, School of Chemistry, University of Leeds, Leeds LS2 9JT, United Kingdom

[§]Department of Mechanical Engineering & Materials Science, Yale University, New Haven, Connecticut 06520, United States

[∥]Department of Physics, Yale University, New Haven, Connecticut 06520, United States

[⊥]Department of Applied Physics, Yale University, New Haven, Connecticut 06520, United States

[#]Department of Cellular and Molecular Physiology, Yale University, New Haven, Connecticut 06510, United States

Supporting Information

ABSTRACT: Recently, a new class of materials emerged with the assembly of DNA-coated phospholipid nanodiscs into columnar BioNanoStacks. Within these stacks, lipid discs are periodically incorporated, resulting into quasi-one-dimensional superstructures. With each disc surrounded by two recombinant scaffolding proteins, we decided to examine whether the polyhistidine tags of these proteins could be utilized to bind additional molecules or particles to these BioNanoStacks. Here we demonstrate that patterning of gold nanoparticles onto these BioNanoStacks is indeed possible. Binding occurs via a nickel-mediated interaction between the nanogolds nitrilotriacetic acid and the histidine tags of the scaffold proteins surrounding the nanodiscs. Using Monte Carlo simulations, we determine that the binding of the nanogold particles to the stacks is not a random event. By comparing the simulation and experimental results, we find that there are preferred binding sites, which affects the binding statistics.

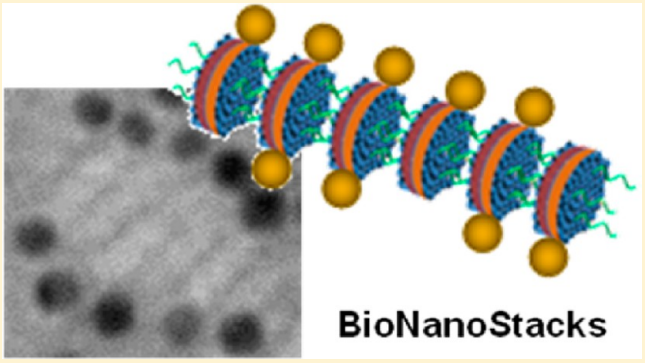

INTRODUCTION

DNA-coated phospholipid nanodiscs have recently emerged as attractive building blocks for programmable organization on the nanometer scale[1] (Figure 1A). Because of the dimensions of the nanodiscs (diameter 10 nm; height ∼5 nm), mixtures of nanodiscs functionalized with complementary DNA assemble into quasi-one-dimensional (1D) strings, named BioNanoStacks (Figure 1B). The BioNanoStacks are unique 1D-assemblies as they provide control on the nanometer scale for both their diameter and the spacing between adjacent discs, without the need of any additional components, or templates, to guide the assembly process.

These three qualities set this whole new class of materials apart from previously studied 1D-assemblies. For β-sheet fibrils[2] and phospholipid−nucleoside[3] assemblies, we do not have the same control of their diameter and periodicity (e.g., helical pitch), as they tend to assemble in a mixture of morphologies. One product 1D-assemblies of inorganic nanoparticles[4] and block copolymers[5] come with a fixed spacing between their periodic units, lacking the additional control in periodicity provided by the DNA linkers of the nanodiscs. The BioNanoStacks are, to our knowledge, the first example of DNA-driven formation of 1D nanostructures that do not require an additionally added single-stranded (ss) DNA to guide, or start, the assembly process.[6,7]

We can extend upon this class of materials by exploiting the potential binding capabilities of the scaffold proteins surrounding the nanodiscs. Within the BioNanoStacks not only the discs are stacked but also their chemical information[1] (e.g., the histidine (His) tags on the proteins; incorporated so the recombinant protein can be purified by immobilized metal ion affinity chromatography[8]). The presence of these binding sites possibly allows these 1D scaffolds to act as templates for metallic patterning. While the nanodiscs are assembled with two scaffold proteins each, every disc contains potentially two binding sites. Addition of metal nanoparticles would enhance the functionality of the BioNanoStacks, as its main components (lipids, proteins, and nucleic acids) generally lack intrinsic functional properties such as sizable conductivity, redox, photoactivity, or magnetic properties.

Metallic patterning could be possible through a nickel (Ni)-mediated interaction between nitrilotriacetic acid (NTA) gold

Received: August 9, 2013
Revised: September 25, 2013
Published: September 27, 2013

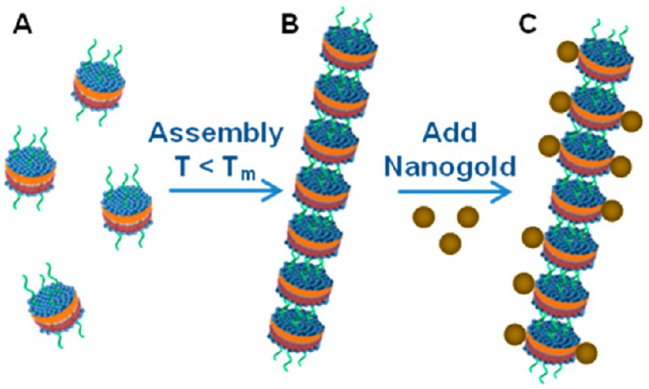

Figure 1. (A) Cartoon depiction of lipid bilayer (blue) nanodiscs stabilized by two MSP1D1 α-helical scaffold proteins (red, orange) and functionalized with lipid–DNA (green). (B) Below the T_m of the DNA duplex, these nanodiscs self-assemble with nanodiscs functionalized with complementary DNA strands to form BioNanoStacks. (C) Addition of Ni-NTA gold nanoparticles leads to patterning of nanogold onto these stacks through binding to the His tags of the scaffolding proteins.

nanoparticles (AuNPs) and the histidines of the scaffolding proteins, as long as these His tags are not buried in the lipid bilayer of the discs, but freely accessible. Earlier work showed that varying the DNA spacer length affects the spacing between discs[1] and thus the spacing between His tags. Therefore, this type of binding could give sub-nanometer control of the spatial separation of the templated Ni–NTA AuNPs (Figure 1C, maximum loading two per disc). The Ni–NTA interaction is site-specific and stable, but unlike a covalent bond it can be easily reversed by adding a competitor like imidazole.[9] While we perform our experiments with nanogold, we note that virtually any molecule can be chemically modified to build in a NTA moiety.[10,11]

Here we report the feasible patterning of Ni–NTA AuNPs onto BioNanoStacks. We observe binding by electron microscopy and track binding patterns by counting the number of gold nearest-neighbors for three types of nanodiscs: discs that have none, one, or a maximum of two Ni–NTA AuNPs attached (Supporting Information Figure S1). In addition, we developed Monte Carlo simulations to determine whether the binding of the Ni-NTA AuNPs to the BioNanoStacks occurs randomly or is affected by steric and energetic interactions between the gold nanoparticles. This paper will demonstrate that His tags on the nanodiscs are capable of binding additional particles, which gives rise to a novel class of materials.

EXPERIMENTAL SECTION

Materials. 1-Palmitoyl-2-oleoyl-*sn*-glycero-3-phosphocholine (POPC) was purchased from Avanti Polar Lipids. The plasmid for bacterial expression of the membrane scaffold protein was obtained from Addgene (Addgene Plasmid 20061: pMSP1D1).[12] Bio beads SM2 were purchased from Bio-Rad. 2-Cyanoethyl *N*,*N*-diisopropyl-chlorophosphoramidite and sodium cholate were purchased from Sigma-Aldrich. 1,2-*O*-Dioctadecyl-*rac*-glycerol was purchased from Chem-Impex. Nano-W negative staining media and Ni-NTA AuNPs (5 nm) were purchased from Nanoprobes, Inc.

MSP1D1 Expression and Purification. The protocol used for expressing and purifying the membrane scaffold protein is based on protocols for expression and purification of membrane scaffold proteins for nanodisc assembly, recently reviewed[13] and described in detail before.[1] Fractions containing MSP1D1 were analyzed for purity by SDS-PAGE gel electrophoresis before being pooled and dialyzed against 20 mM Tris/HCl, 0.1 M NaCl (pH 7.4). Protein concentrations were measured by UV absorption at 280 nm and concentrated to approximately 150–250 μM by ultracentrifugation filtration.

DNA–Lipid Synthesis. Synthesis of DNA–lipid conjugates has been described previously.[1,14,15] We used lipid–DNA conjugates with the following four base sequences: dioctadecyl lipid-5′-TTT ACA GAC TAC C-3′ (LDNA1), dioctadecyl lipid-5′-TTT GGT AGT CTG T-3′ (LDNA2), dioctadecyl lipid-5′-TTT CGG GGA CAG TAC AGA CTA CC-3′ (LDNA3), and dioctadecyl lipid-5′-TTT GGT AGT CTG TAC TGT CCC CG-3′ (LDNA4). Successful lipid–DNA conjugation was checked by mass spectroscopy.[1] Lipid–DNA concentrations in solution were determined by UV adsorption at 260 nm.

Assembly of Lipid Nanodiscs. Detailed protocols for reconstitution of lipid nanodiscs have been reported.[8] Here we followed the same preparation method as described earlier.[1] DNA–lipids were added to aliquots of the nanodisc sample to yield a final mean loading of 4 DNA per nanodisc. Lipid–DNA and nanodiscs were then incubated by gently shaking for at least 45 min at 4 °C to allow the lipid–DNA conjugates to diffuse into the nanodiscs.

Thermal BioNanoStack assembly (Monitored by UV–vis Adsorption Spectroscopy). BioNanoStacks are formed by slow cooling of mixed populations of functionalized nanodiscs. Equivalent proportions of LDNA1 and LDNA2 (or LDNA3 and LDNA4) functionalized nanodiscs are mixed at a final nanodisc concentration of 4 μM. The samples are then rapidly heated to 60 °C in a Cary 100 Biomelt UV–vis spectrophotometer (Agilent Technologies) and kept at that temperature for 5 min. Then, the samples are slowly cooled at −0.1 °C/min to room temperature to allow the DNA-functionalized nanodiscs to self-organize into near-equilibrium superstructures.

Samples were degassed prior to analysis and prepared in stoppered quartz semi-microcuvettes. UV adsorption at 320 nm, a wavelength at which DNA does not adsorb, was monitored during thermal cycling to detect assembly and disassembly of superstructures through turbidity changes in the sample.

AuNPs Binding to BioNanoStacks (Monitored by Transmission Electron Microscopy). BioNanoStacks were diluted to 0.2 μM in a 50 mM NaCl buffer. 40 μL of Ni-NTA AuNPs (0.5 μM; diameter 5 nm) was added to a droplet (40 μL) of sample (estimated 2.5:1 AuNPs:discs). After 3 min a transmission electron microscopy (TEM) grid (carbon-coated Formvar) is placed on top of this solution for 2 min. The grid is then placed on a droplet of 2% Nano-W staining solution for 4 min before wicking away excess liquid on a piece of blotting paper. TEM images to observe AuNPs binding to the BioNanoStack scaffolds were obtained using a FEI Tenai Biotwin 80–120 kV TEM. The incubation time for the AuNPs with BioNanoSacks was increased for 12 h without a noticeable difference in gold coverage.

AuNPs Binding to BioNanoStacks (Monitored by Cryo-TEM). Cryo-TEM samples were obtained using a FEI Tecnai F20 TWIN electron microscope at 200 kV acceleration voltage, using a nominal magnification of 50 000. We recorded images on a 4k × 4k CCD camera (Gatan) at a pixel size of 1.74 Å using low-dose mode with an exposure dose of 13–18 e Å^{-2}. The images are taken with three defocus values, −1.5, −4.5, and −15 μm, and merged into one by phase-flipping and image processing. Commercially available holey carbon grids, C-flat 2/2 4C (Protochips) covered with homemade thin carbon film (5 nm), were glow-discharged before use. BioNanoStacks (4 μM in 50 mM NaCl and 10 mM TRIS) were incubated with three concentrations (~ Au:disc 0.5:1, 2.5:1, and 4:1) of AuNPs and given 30 s to adsorb to the grids; the samples were blotted for 3 s at −0.5 mm offset in 100% humidity at 8 °C and flash frozen in liquid ethane using an FEI Vitrobot.

Monte Carlo Computer Simulations. We developed Monte Carlo simulations of a collection of N stacks containing n_i nanodiscs, where i = 1 to N, to investigate nanodisc binding. Each disc has two binding sites. A constant number (p = 0.55) of gold atoms n_g with occupation fraction $p = n_g/(2\sum n_i)$ is used, where p = 0 indicates no binding (all binding sites are free) and p = 1 means that there every site, two per disc, is occupied. We assume that adjacent AuNPs have a

dx.doi.org/10.1021/la403091w | *Langmuir* 2013, 29, 13089–13094

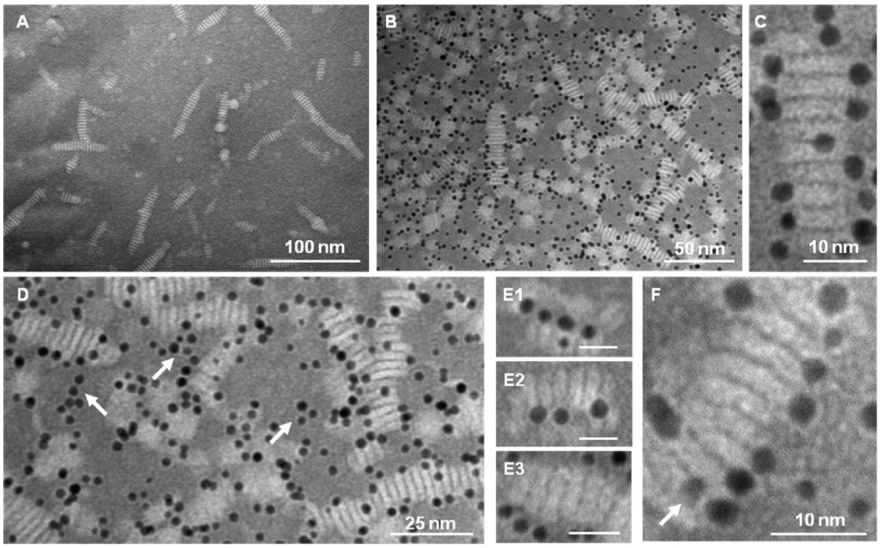

Figure 2. TEM micrographs of BioNanoStacks after negative staining with Nano-W. (A) 400 nM mixed population of POPC nanodiscs with a mean DNA loading of 4 per nanodisc (LDNA1 or LDNA2) assembled in a 50 mM NaCl buffer. (B) 1 mM population of POPC nanodiscs with a mean DNA loading of 4 per nanodisc (LDNA1 or LDNA2) assembled in a 50 mM NaCl buffer after a 3 min incubation with 5 nm gold NTA nanoparticles. (C) Zoom-in on a BioNanoStack decorated with AuNPs. (D) Further increase of the concentration of gold leads to unbound particles surrounding the BioNanoStacks. (E1−E3) AuNPs are mostly found on top, in the middle (1), on one side of the stack (2), or both sides of the stacks (3); scale bars = 10 nm. (F) Zoom-in on a BioNanoStack decorated with AuNPs to show a rare case of two AuNPs in close vicinity of one side of the stack (arrow).

binding energy penalty of ε. Thus, placing an AuNP on a nanodisc at binding site k with 0 gold neighbors has an energy penalty of $E_k = \varepsilon_0$, whereas 1 gold neighbor has a penalty of $E_k = \varepsilon_1$, and 2 gold neighbors has a penalty of $E_k = \varepsilon_2$.

For the Monte Carlo updates, we first randomly selected a nanodisc site i without a bound AuNP and a nanodisc site j with one bound AuNP. The AuNP is moved from site j to i with probability $e^{E_k/T}$, where T (in units of the Boltzmann constant k_B) is the temperature of the system. The temperature T was decreased nearly quasi-statically as $T(t) = 100e^{-t/\tau}$ where t is the number of Monte Carlo steps and $\tau = 4.3 \times 10^8$ is the decay constant, and averages were calculated over more than 10^7 Monte Carlo steps. We calculate the probability P_{kl} of a nanodisc with k gold atoms having l neighbors, where $k = 0, 1, 2$ and $l = 0, 1, 2, 3, 4$, excluding nanodiscs on the ends of the stacks. We compared results from this model to one where AuNPs were randomly placed on nanodisc binding sites, which corresponds to $T = \infty$.

To compare simulation and experimental results, we measured the deviation between the binding probabilities $\Delta^2 = A\sum_{i=0}^{2}\sum_{j=0}^{4}(P_{ij}^{sim} - P_{ij}^{exp})^2$, where P_{ij}^{sim} (P_{ij}^{exp}) are the simulation (experimental) probabilities of a site with i AuNPs with j neighbors, and Δ is normalized so that $\Delta = 0$ when simulation and experiment perfectly overlap ($P_{ij}^{sim} = P_{ij}^{exp}$ for all i and j) and $\Delta = 1$ when simulation and experiment are maximally mismatched (i.e., $A = 1/6$).

RESULTS AND DISCUSSION

To obtain BioNanoStacks scaffolds, a stoichiometric mixture (4 μM) of complementary functionalized DNA-coated nanodiscs was mixed and allowed to assemble into stacks by slowly cooling (−0.1 °C/min) from 60 °C (a temperature at which the DNA strands do not hybridize[16] and the nanodiscs are known to be stable[17]) to room temperature in a Cary 100 Biomelt UV−vis spectrophotometer. Negative-staining transmission electron microscopy (TEM; stained with Nano-W, Nanoprobes, Inc.) confirmed the nanodisc stacking structure through hybridization of complementary DNA functionalities (Figure 2A). The experiments were performed with 13 base long LDNA1 (lipid-5′-TTT ACA GAC TAC C-3′) and LDNA2 (lipid-5′-TTT GGT AGT CTG T-3′).

Figure 2B clearly shows that the His tags of the BioNanoStacks are capable of binding Ni-NTA AuNPs. AuNP binding is observed on all BioNanoStacks, although individual nanodiscs show differences in the number of particles bound. To obtain this result, Ni-NTA AuNPs (0.5 μM; further referred to as AuNPs) were added in a 1:1 ratio (volume ∼ 2.5:1 Au:disc) to a solution of assembled lipid nanodiscs (0.2 μM) and incubated for 3 min (longer incubation times, up to 12 h, did not affect the results). Binding of AuNPs was monitored with negative-staining TEM. To our knowledge, this is the first time the His tags of the scaffold proteins have been used for more than a purification purpose.

BioNanoStacks with a relative high number of bound AuNPs (Figure 2C) are never filled to full capacity. Each lipid nanodisc contains two scaffold proteins. One His tag per protein results in a maximum of two AuNPs per disc. Further increasing the concentration of AuNPs did not result in an increase in binding; BioNanoStacks are already surrounded by unbound particles at the concentration we employed (Figure 2D, arrows). The BioNanoStacks studied had 55% of their binding sites occupied by an AuNP.

The binding of the AuNPs on the BioNanoStacks takes place in two dominate orientations. The binding occurs either across the middle or on the flanks of the stacks (Figure 2E1−3). Only rarely are particles found in other orientations (Figure 2F, arrow). As the binding spot of the nanogold correlates with the position of the His tags of the scaffold proteins, this may hint to a preference in protein orientation, resulting in His tag display on opposing sites of the disc. Preferential orientations could be caused by drying effects or by an attraction between the AuNPs and the TEM grids.

To remove the possibility of potential drying artifacts in the observed preferred orientation of the AuNPs bound to BioNanoStack, cryo-TEM was used (Figure 3A−C). Experiments were conducted at three different AuNPs concentrations (∼ Au:disc 0.5:1, 2.5:1, and 4:1). Figure 3A shows that AuNPs

dx.doi.org/10.1021/la403091w | Langmuir 2013, 29, 13089−13094

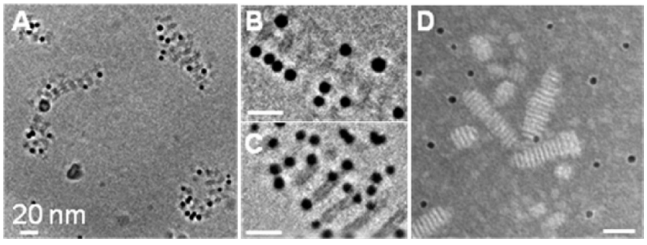

Figure 3. Control experiments on AuNP and BioNanoStack binding. (A) Cryo-TEM image of AuNPs binding to BioNanoStacks. (B, C) Zoom-in on BioNanoStacks imaged with cryo-TEM. Even without drying effects, the AuNPs seem to prefer binding on opposite sides of the stacks. (D) Gold nanoparticles lacking a Ni–NTA coating are unable to bind to BioNanoStacks. All scale bars are 20 nm.

bind to the BioNanoStacks. The AuNPs bound are found along the flanks of the stacks. To determine if these binding sites are predominantly present at the flanks, or if these are the most accessible, two higher concentrations of AuNPs were examined as well. Figure 3B shows a BioNanoStack with a higher coverage of AuNPs. Addition of more AuNPs results in free AuNPs surrounding the stacks. Note that the 180° orientation is again dominant in these images. While this raises an interesting point, the mechanism is beyond the scope of this work.

Binding specificity of AuNPs to the BioNanoStacks is confirmed with two control experiments. First, gold nanoparticles of similar size but with a different coating (a-specific; protein A) were tested for their ability to bind. Figure 3C shows that, in contrast to the Ni–NTA particles, the protein A-coated gold nanoparticles are not capable of binding to the BioNanoStacks. The importance of the Ni–NTA group is further confirmed by using imidazole to remove bound AuNPs by competing for their binding sites. The BioNanoStacks with bound AuNPs were exposed to imidazole solutions of different concentrations. BioNanoStack binding site occupation decreased from 55% for no imidazole exposure to 25% after 1 min incubation in 50 mM imidazole and 6% after 1 min incubation in 250 mM imidazole (data not shown).

AuNP binding was further examined by a statistical analysis of the data to determine which types of binding patterns occurred most often. First each disc (self; s) was divided into one of three types: discs with no, one, or two bound AuNPs (cartoons in Figure 4). Within our samples of BioNanoStacks, 15% of the discs had zero, 60% had one, and 25% had two AuNPs attached. To look beyond the particles directly bound to a certain disc, we subsequently compared the amount of particle nearest neighbors (n) surrounding the three disc types. As every disc can have two particles bound, the maximum number of AuNPs is four (see Supporting Information Figure S1 for examples). For each stack, the first and last disc were omitted from the count as self (as these can have only a maximum of two nearest neighbors), but included for neighboring particle counts for the second and next to last discs. Over 1000 discs of three independently prepared samples were counted and scored in this manner. As we found no significant variation between samples, the total results are plotted together (Figure 4, bars).

Two binding trends are clear from Figure 4: (1) the probability of 0 nearest neighbors increases with increasing colloids (self) per disc, and (2) the probability of 3 nearest neighbors decreases with increasing colloids per disc.

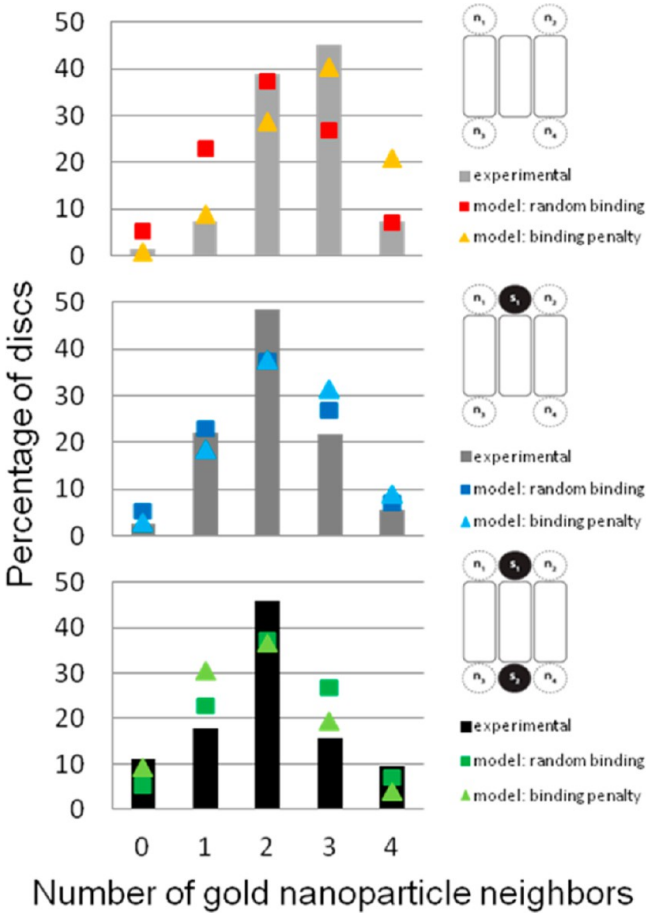

Figure 4. Percentage of discs found with a given number of AuNP nearest neighbors (zero (top), one (middle), or two (bottom)): bars: experimental results; squares: Monte Carlo simulation results assuming random AuNP binding; triangles: Monte Carlo simulation results including binding penalties for neighboring AuNPs.

The two binding trends suggest that AuNP binding to BioNanoStacks is not a strictly random event, but the overall shapes of the distributions do not disclose a clear binding strategy. While we use AuNPs that are close in size to the thickness of the nanodiscs (5 nm vs 5.7 nm), the indication of steric effects is not surprising. To better understand the binding behavior, we performed Monte Carlo simulations. As a control, we first implemented an "uncorrelated model", where AuNPs bind to any spot without constraints. We also implemented a "correlated model" with a binding penalty when AuNPs bind to sites with adjacent AuNPs.

In the Monte Carlo simulations, we calculated the probability $e^{-E_k/T}$ of moving an AuNP from an occupied site to an open binding site. For the random system, we set the temperature of the system to infinity, which implies that each site is equally probable for binding. Figure 4 shows that random particle binding does not match the experimental results. In the random case (Figure 4, squares), the data are similar for the three disc types, which is not observed in the experimental results. Also, for the random model, we find $\Delta = 0.125$, which means that simulations and experiment match by only 87.5%.

We also performed Monte Carlo simulations over a range of temperature with binding penalties (when binding sites have neighboring AuNPs) that were selected so that the binding probabilities best match those from experiment. The best

dx.doi.org/10.1021/la403091w | Langmuir 2013, 29, 13089–13094

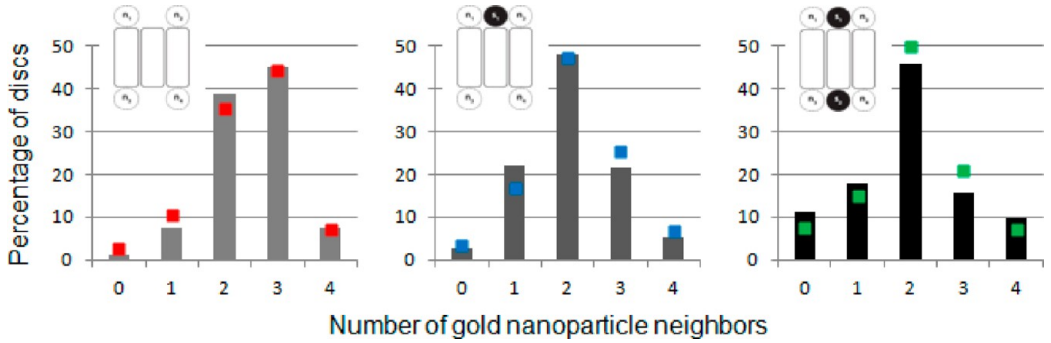

Figure 5. Experimental results of percentages of discs with a given number of gold (Au) nanoparticle neighbors for discs with either zero (left), one (middle), or two (right) gold nanoparticles bound. The BioNanoStacks are assembled with the longer 23-mer DNA linkers. Dots: experimental results of gold nanoparticle patterning on the 13-mer DNA assembled BioNanoStacks.

match to experiments was $\varepsilon_0 = 10T$, $\varepsilon_1 = 10T$, and $\varepsilon_2 = 50T$ for 0, 1, and 2 AuNP neighbors, respectively (Figure 4, triangles). Especially for discs without AuNP (top graph), the improvement over the random model is clear. Our results show that for a model with binding energy penalties we increase the match between simulation and experiment from 87% to more than 93% ($\Delta = 0.066$).

To fine-tune the agreement between the experimental data and Monte Carlo simulation results, we introduced an additional energy penalty for next nearest neighbors. We ran Monte Carlo simulations over a large range of nearest-neighbor and next-nearest-neighbor binding penalties, but this modification did not improve the agreement between experimental data and simulation results ($\Delta = 0.066$, data not shown). We can also imagine the binding of one AuNP to two neighboring nanodiscs, as the numerous Ni−NTA groups can bind more than one His tag. Thus, an even more quantitatively accurate model would include the blocking of a fraction of the binding sites.

From the Monte Carlo simulations and experimental data, it is clear that if complete AuNP coverage is the goal, we need to decrease the binding penalty. We anticipate that the binding penalty is a result of a combination of several factors. These include the steric and electrostatic interactions between the AuNPs, the possible blocking of binding sites due to the close proximity of the His tags on adjacent nanodiscs, or the orientation of the two proteins (His tags) on one nanodisc. One option to improve the AuNP coverage is to increase the spacing between the nanodiscs within the BioNanoStack. The periodicity between the discs can be adjusted by increasing the spacing with longer DNA linkers. To test this hypothesis, we repeated the experiments on BioNanoStacks assembled with LDNA3 (lipid-5′-TTT CGG GGA CAG TAC AGA CTA CC-3′) and LDNA4 (lipid-5′-TTT GGT AGT CTG TAC TGT CCC CG-3′). The results (Figure 5, bars) are very similar to those in Figure 4 (and plotted in Figure 5, squares). We speculate that a difference in AuNP binding is lost upon drying onto the TEM grids, but an even larger spacing between individual discs could improve the coverage of AuNPs onto BioNanoStacks.

Other options that could decrease the binding penalty include increasing the diameter of the nanodiscs[18] (decreasing the probability of one AuNP binding to the His tags of two neighboring nanodiscs), reducing the size of the AuNPs, adding a coating that reduces the friction among neighboring particles, or adjusting the salt concentration to better screen against short-range electrostatic repulsions. Complete AuNP coverage would improve methods to create nanowires but could potentially turn out to be an elusive structure. It may be that instead of having a population of BioNanoStacks with all its His tags in the 180° orientation, part of these stacks actually have both their His tags at the same angular orientation (0° orientation).[19] The latter orientation results in fewer discs with 2 AuNPs bound, not because the site is blocked, or sterically hindered, but because a nanodisc with its proteins (His-tags) in this angular orientation essentially can only bind one AuNP.

Nevertheless, we anticipate that complete NP coverage is not necessary for these novel hybrid materials to be useful within several exciting applications. One promising area is the utilization of the BioNanoStacks as potential drug delivery vehicles. Not only are the nanoscale dimensions and biodegradability of these structures highly desirable, but due to their nonspherical symmetry they could have favorable interactions with cell surfaces that favor their internalization through cell uptake pathways and improved hydrodynamic properties within circulatory blood flow.[20] Furthermore, inclusion of integral membrane proteins or therapeutic compounds or growth factors into nanodiscs[21] may allow new opportunities in drug delivery. Future studies will also include the possible patterning of other metal NPs for applications in catalysis, nanoelectronics, and nanophotonics.

■ CONCLUSIONS

BioNanoStacks are promising for many applications in materials and device design. The three basic materials (lipids,[22] proteins,[23] and DNA[24,25]) that form these structures provide a variety of available strategies for incorporation of additional functionalities into BioNanoStack architectures. Here we tested one of these possibilities: utilizing the His tags of scaffold proteins to attach AuNPs. We determined that while the protein His tags are open and available for particle binding, there are steric or energetic effects that prevent complete coverage. Nevertheless, the option of extending BioNanoStacks with additional AuNPs is an exciting finding. Because of the generic Ni−NTA−His-tag linkage, the same method can be used for patterning BioNanoStacks with other molecules or particles of interest.

■ ASSOCIATED CONTENT

Supporting Information

TEM images of all example binding patterns of nanogold to BioNanoStacks. This material is available free of charge via the Internet at http://pubs.acs.org.

dx.doi.org/10.1021/la403091w | *Langmuir* 2013, 29, 13089−13094

AUTHOR INFORMATION

Corresponding Author

*E-mail: kyle.vanderlick@yale.edu (T.K.V.).

Notes

The authors declare no competing financial interests.

ACKNOWLEDGMENTS

C.O. and C.S. acknowledge partial support from NSF MRSEC DMR-1119826. We thank Dr. Jin Nam for assistance with the lipid phosphoramidite synthesis, the group of Corey Wilson for MSP1D1 purification, and Morven Graham at the electron microscopy facility at the Yale School of Medicine for supplying us with protein A-coated nanogold. We also acknowledge Prof. Fred Sigworth for helpful discussions on cryo-TEM.

REFERENCES

(1) Beales, P. A.; Geerts, N.; Inampudi, K. K.; Shigematsu, H.; Wilson, C. J.; Vanderlick, T. K. Reversible assembly of stacked membrane nanodiscs with reduced dimensionality and variable periodicity. *J. Am. Chem. Soc.* **2013**, *135*, 3335−3338.

(2) Jimenez, J. L.; Nettleton, E. J.; Bouchard, M.; Robinson, C. V.; Dobson, C. M.; Saibil, H. R. The protofilament structure of insulin amyloid fibrils. *Proc. Natl. Acad. Sci. U. S. A.* **2002**, *99*, 9196−9201.

(3) Yanagawa, H.; Ogawa, Y.; Furuta, H.; Tsumo, K. Spontaneous formation of superhelical strands. *J. Am. Chem. Soc.* **1989**, *11*, 4567−4570.

(4) Li, M.; Schnablegger, H.; Mann, S. Coupled synthesis and self-assembly of nanoparticles to give structures with controlled organization. *Nature* **1999**, *240*, 393−395.

(5) Cui, H.; Chen, Z.; Zhong, S.; Wooley, K. L.; Pochan, D. J. Block copolymer assembly via kinetic control. *Science* **2007**, *317*, 647−650.

(6) Lo, P. K.; Karam, P.; Aldaye, F. A.; McLaughlin, C. K.; Hamblin, G. D.; Cosa, G.; Sleiman, H. F. Loading and selective release of cargo in DNA nanotubes with longitudinal variation. *Nat. Chem.* **2010**, *2*, 319−328.

(7) Janssen, P. G.; Brankaert, N. J. M.; Vila, X.; Schenning, P. H. J. ssDN templated assembly of oligonucleotides and bivalent napthalene guests. *Soft Matter* **2010**, *6*, 1494−1502.

(8) Hochuli, E.; Bannwarth, W.; Dobeli, H.; Gentz, R.; Stuber, D. Genetic approach to facilitate purification of recombinant proteins with a novel metal chelate adsorbent. *Nat. Biotechnol.* **1988**, *6*, 1321−1325.

(9) Lata, S.; Reichel, A.; brock, R.; Tampe, R.; Piehler, J. High-affinity adaptors for switchable recognition of histidine-tagged proteins. *J. Am. Chem. Soc.* **2005**, *127*, 10205−10215.

(10) Maly, J.; Meo, C. D.; De Francesco, M.; Masci, A.; Masojidek, J.; Sugiura, M.; Volpe, A.; Pilloton, R. Reversible immobilization of engineered molecules by Ni-NTA chelators. *Bioelectrochemistry* **2004**, *63*, 271−275.

(11) Goodman, R. P.; Erben, C. M.; Malo, J.; Ho, W. M.; McKee, M. K.; Kapandis, A. N.; Tuberfield, A. J. A facile method for reversibly linking a recombinant protein to DNA. *ChemBioChem* **2009**, *10*, 1551−1557.

(12) Denisov, I. G.; Grinkova, Y. V.; Lazarides, A. A.; Sligar, S. G. Directed self-assembly of monodisperse phospholipid bilayer nanodiscs with controlled size. *J. Am. Chem. Soc.* **2004**, *116*, 3477−3487.

(13) Ritchie, T. K.; Grinkova, Y. V.; Bayburt, T. H.; Denisov, I. G.; Zolnerciks, J. K.; Atkins, W. M.; Sligar, S. G. Reconstitution of membrane proteins in phospholipid bilayer nanodiscs. *Methods Enzymol.* **2009**, *464*, 211−231.

(14) Beales, P. A.; Nam, J.; Vanderlick, T. K. Specific adhesion between DNA-functionalized "Janus" vesicles: size-limited clusters. *Soft Matter* **2011**, *7*, 1747−1755.

(15) Chan, Y.-H. M.; van Lengerich, B.; Boxer, S. G. Lipid-anchored DNA mediates vesicle fusion as observed by lipid and content mixing. *Biointerphases* **2008**, *3*, FA17−21.

(16) Beales, P. A.; Vanderlick, T. K. DNA as Membrane-bound ligand-receptor pairs: duplex stability is tuned by intermembrane forces. *Biophys. J.* **2009**, *96*, 1554−1565.

(17) Shaw, A. W.; McLean, M. A.; Sligar, S. G. Phospholipid phase transitions in homogeneous nanometer scale bilayer discs. *FEBS Lett.* **2004**, *556*, 260−264.

(18) Ritchie, T. K.; Grinkova, Y. V.; Bayburt, T. H.; Denisov, I. G.; Zolnerciks, J. K.; Atkins, W. M.; Sligar, S. G. Reconstitution of membrane proteins in phospholipid bilayer nanodiscs. *Methods Enzymol.* **2009**, *464*, 211−231.

(19) Frauenfeld, J.; Gumbart, J.; Sluis, E. O.V.D.; Funes, S.; Gartmann, M.; Beatrix, B.; Mielke, T.; Berninghausen, O.; Becker, T.; Schulten, K.; Beckmann, R. Cryo-EM structure of the ribosome-SecYE complex in the membrane environment. *Nat. Struct. Mol. Biol.* **2011**, *18*, 614−621.

(20) Simone, E. A.; Dziubla, T. D.; Muzykantov, V. R. Polymeric carriers: role of geometry in drug delivery. *Expert Opin. Drug Delivery* **2008**, *5*, 1283−1300.

(21) Bayburt, T. H.; Sligar, S. G. Membrane protein assembly into nanodiscs. *FEBS Lett.* **2010**, *584*, 1721−1727.

(22) Zhang, X.-X.; McIntosh, T. J.; Grinstaff, M. W. Functional lipids and lipoplexes for improved gene delivery. *Biochimie* **2012**, *94*, 42−58.

(23) Basle, E.; Joubert, N.; Pucheault, M. Protein chemical modification on endogenous amino acids. *Chem. Biol.* **2010**, *17*, 213−227.

(24) Jager, S.; Rasched, G.; Kornreich-Leshem, H.; Engeser, M.; Thum, O.; Famulok, M. A versatile toolbox for variable DNA functionalization at high density. *J. Am. Chem. Soc.* **2005**, *127*, 15071−15082.

(25) Pinheiro, A. V.; Han, D.; Shih, W. M.; Yan, H. Challenges and opportunities for structural DNA nanotechnology. *Nat. Nanotechnol.* **2011**, *6*, 763−772.